Thermodynamics of Fab−ssDNA Interactions: Contribution of Heavy Chain Complementarity Determining Region 3†

Andrey A. Komissarov‡ and Susan L. Deutscher*

Department of Biochemistry, University of Missouri School of Medicine, Columbia, Missouri 65212

Received June 11, 1999; Revised Manuscript Received August 27, 1999

ABSTRACT: The recombinant anti-ssDNA Fab, DNA-1, and 16 heavy chain complementarity determining region 3 (HCDR3) mutant variants were selected for thermodynamic characterization of ssDNA binding. The affinity of Fab to $(dT)_{15}$ under different temperatures and cation concentrations was measured by equilibrium fluorescence quenching titration. Changes in the standard Gibbs free binding energy ($\Delta G°$), enthalpy ($\Delta H°$), entropy ($\Delta S°$), and the number of ionic pairs (Z) formed upon interaction were determined. All Fab possessed an enthalpic nature of interaction with ssDNA, that was opposite to the previously reported entropically driven binding to dsDNA [Tanha, J., and Lee, J. S. (1997) *Nucleic Acids Res. 25,* 1442−1449]. The contribution of separate residues of HCDR3 to ssDNA interaction was investigated. Analysis of the changes in $\Delta H°$ and $T\Delta S°$, induced by substitutions in HCDR3, revealed a complete entropy/enthalpy compensation. Mutations R98A and D108A at the ends of the HCDR3 loop produced increases in $T\Delta S°$ by 10.4 and 15.9 kcal/mol, respectively. Substitution of proline for arginine at the top of HCDR3 resulted in a new electrostatic contact with $(dT)_{15}$. The observed linear correlation of Z and $\Delta G°$ of nonelectrostatic interactions ($\Delta G°_{nonel}$) at the anti-ssDNA combining site was used for the estimation of the specific $\Delta G°_{nonel}$ [−20 to −25 cal/(mol·Å^2)], the average contact area (450−550 Å^2), the maximal Z (6−7), and the limit in affinity under standard cation concentrations [$(0.5-1) \times 10^8$ M^{-1}] for this family of Fab. Results suggested that rational engineering of HCDR3 could be utilized to control the affinity and likely the specificity of Ab−DNA interactions.

Given their essential roles in gene regulation, DNA−protein complexes have been the subject of numerous structure and function studies. In contrast to other types of DNA-binding proteins, anti-DNA antibodies (Abs)[1] are unique in that they possess a similar structural organization of the combining site that is comprised of small variable regions that dictate affinity and specificity, contained in a rigid framework of conserved constant domains *(1)*. The antigen combining site consists of three hypervariable complementarity determining regions (CDRs) in each of the two heavy (H) and light (L) chains. Two types of anti-DNA Abs, anti-ssDNA and anti-dsDNA, are of particular interest since they are produced in vivo in autoimmune disease patients *(2)*. The presence of anti-dsDNA Abs in sera is diagnostic of the autoimmune disease systemic lupus erythematosus (SLE) *(3)*. More importantly, many pathologic consequences of SLE have been linked to the production and deposition of anti-dsDNA Ab immune complexes *(4, 5)*. While anti-ssDNA Abs have been identified in diseased tissue *(6)*, their role in autoimmunity remains uncertain *(3)*.

Results of X-ray crystallographic experiments and molecular modeling have demonstrated that structural differences in DNA can determine the type of interaction pattern between the Ab and DNA and the shape of the interface *(7, 8)*. Ab−ssDNA combining sites have been shown to form a deep cleft where the ligand is bound *(9, 10)*. In contrast, the contact areas formed with dsDNA *(11)* and triple-stranded DNA *(12)* are usually more flat and contain more electrostatic contacts compared to Ab−ssDNA complexes. The structures of anti-DNA Abs available *(7−13)* indicate that their contact areas are considerably smaller than those of other DNA-binding proteins *(14)*. While structural data have yielded information on combining site architecture and contact residues, they have not improved an understanding of the dynamics involved in complex formation or the differences in pathogenic and nonpathogenic anti-DNA Abs. Presently, only thermodynamic studies of dsDNA−Ab complex formation have been reported. The binding of the anti-dsDNA Abs Jel 241 and Jel 274 to dsDNA was shown to be strictly entropy-driven and highly dependent on salt concentration *(15)*.

Despite differences in combining site structures, HCDR3 of both anti-ssDNA *(16−19)* and anti-dsDNA *(20−22)* Abs has been shown to play a key role in determining affinity and, perhaps, specificity of interaction. HCDR3 contains the most sequence variability and forms a loop of which the top is generally involved in direct antigen interaction and the

† This work was supported by National Institutes of Health Grant GM-47979 and by a University of Missouri Research Board Grant (to S.L.D.).

* Corresponding author: Department of Biochemistry, M121 Medical Sciences Building, University of Missouri School of Medicine, Columbia, MO 65212. Telephone: 573-882-2454. Fax: 573-884-4597. E-mail: deutschers@missouri.edu.

‡ Present address: Henry Ford Health Sciences Center, One Ford Place, 5D, Detroit, MI 48202.

[1] Abbreviations: Ab, antibody; CDR, complementarity determining region; Fab, antigen-binding fragment(s); H, heavy chain; L, light chain; SLE, systemic lupus erythematosus.

10.1021/bi991347l CCC: $18.00
Published on Web 10/12/1999

end residues are buried and may act to support the conformation as a whole *(23−25)*.

An anti-ssDNA Fab, DNA-1, that was previously selected from a bacteriophage display library generated from an autoimmune mouse *(26)*, was chosen for examination of the thermodynamic mechanisms of ssDNA interaction. The binding properties of DNA-1 to ssDNA have been intensely examined, and a molecular model and a set of HCDR3 mutants were previously generated *(18, 19, 27−29)*. These ssDNA-binding Fab possessed a wide range of affinities, and facilitated the study of both the mechanism of ligand recognition and the influence of a mutation on ssDNA−Fab association. Equilibrium fluorescence quenching titration was used for measurements of association constants of DNA-1 and 16 HCDR3 mutants to $(dT)_{15}$ under different temperatures and cation concentrations. Results obtained for DNA-1 and the HCDR3 mutants together with data published for other anti-ssDNA Abs allowed for exploration of the general features of ssDNA−Fab interactions. A comparison of the thermodynamics of Fab−ssDNA versus Fab−dsDNA interaction may uncover the mechanism of recognition of different species of DNA. Ultimately, these results may help decipher the fundamental basis of the pathogenicity of anti-DNA Abs.

MATERIALS AND METHODS

Reagents. Ni−NTA agarose was purchased from Qiagen Corp. (Chatsworth, CA); Gamma-bind Sepharose, a Mono-S FPLC column, and poly(dT) were obtained from Pharmacia Biotech (Piscataway, NJ); and other reagents were from Fisher Scientific (St. Louis, MO) or Sigma Chemical Co. (St. Louis, MO). Oligonucleotides were synthesized by the University of Missouri DNA Core Facility and exhibited greater than 99% purity by analytical HPLC.

Expression and Purification of DNA-1 and HCDR3 Mutants. The Fab were isolated by affinity chromatography and cationic exchange FPLC as described *(19)*. All Fab were homogeneous in accordance with SDS−polyacrylamide gel electrophoresis and demonstrated a A_{280}/A_{260} ratio of more than 1.90 *(30)*. Protein concentration was determined either by reaction with bicinchoninic acid *(31)* or calculated from absorbance at 280 nm *(29)*.

Fluorescence Titration. Equilibrium fluorescence quenching titrations were carried out using an SLM 8100 spectrofluorimeter with an excitation wavelength of 292 nm and an emission wavelength of 346 nm *(19)*. The temperature of the reaction mixture cell compartment was controlled with an accuracy of ±0.1 °C within the range of 25−50 °C as described *(19)*. All titrations were performed with varying amounts of oligonucleotide added to a fixed Fab concentration (5−50 nM) in 2 mL of 50 mM Tris-HCl buffer, pH 7.0, in a 1 cm path length cuvette. Binding isotherms were fitted to the observed fluorescence quenching values using a one-site equilibrium model for binding *(19)*.

Salt-Back Fluorescence Titration. Certain association constant (K_a) values were determined by salt-back titrations *(32, 33)*. Since the free Fab fluorescence was known and the maximal fluorescence (F_{max}) was independent of NaCl concentration, the concentration of bound Fab ($[Fab]_b$) could be calculated from the ratio of F_{obs}/F_{max} at each value of salt concentration as $[Fab]_b = F_{obs}[Fab]_t/F_{max}$, where $[Fab]_t$ was the total Fab concentration. Thus, K_a for each salt concentration was calculated as

$$K_a = [Fab]_b/[Fab]_f[(dT)_{15}]_f$$

where $[Fab]_f = [Fab]_t - [Fab]_b$ and $[(dT)_{15}]_f = [(dT)_{15}]_t - [Fab]_b$.

van't Hoff Analysis of Fab−$(dT)_{15}$ Interactions. Fab affinities to $(dT)_{15}$ were measured in 50 mM Tris-HCl, pH 7.0, at temperatures ranging from 25 to 50 °C. The temperature dependence of the pK_a of Tris was corrected using the coefficient of −0.031 pH unit/deg *(34)*. Values of the standard binding enthalpy ($\Delta H°$) were determined from the slopes of dependencies of ln K_a versus $1/T$ using the differential van't Hoff equation. Changes in the standard Gibbs free binding energy ($\Delta G°$) at 25 °C were calculated for every Fab as $\Delta G° = -RT \ln K_a$, where $R = 1.987$ cal/mol. Values of the changes in the standard binding entropy ($\Delta S°$) were found as $-T\Delta S° = \Delta G° - \Delta H°$.

Salt Dependence of Affinity of Fab to $(dT)_{15}$. The K_a values for Fab−$(dT)_{15}$ complexes were measured by direct and salt-back fluorescence quenching titration at 25 °C in 50 mM Tris-HCl, pH 7.0, with addition of 10−500 mM NaCl. The numbers of ionic pairs formed between Fab and $(dT)_{15}$ (Z) were estimated for DNA-1 and the HCDR3 mutant variants from the linear dependencies of ln K_a on ln $[Cat^+]$ using the equation: $\ln K_a = \ln K_a^o - Z\psi \ln [Cat^+]$ *(35)*, where ψ was the number of cations released from the oligonucleotide for each pair formed [$\psi = 0.76-0.78$ for oligo(dT)] *(36, 37)*, $[Cat^+]$ was the sum of the concentrations of Na^+ and Tris, and K_a^o was the association constant under standard cation concentration (1 M). Values of $\Delta G°_{1M}$ were calculated as $-RT \ln K_a^o$.

RESULTS

DNA-1 and HCDR3 Mutants as a Model for the Study of the Molecular Mechanism of Fab−ssDNA Interactions. DNA-1 *(26)*, and a set of its mutant variants *(29)*, formed a unique group of recombinant anti-ssDNA Fab with different affinities induced by known amino acid alterations in HCDR3. Sixteen Fab with a 2 order magnitude range in affinities were selected for the present study. Thirteen of them contained mutations at the top of HCDR3 (^{101}Tyr-Arg-Pro-Tyr-Tyr^{105}). Three other Fab (R98A, D108A, and R98A/D108A) had mutations of the charged residues at the ends of the HCDR3 loop, and, with DNA-1, formed a double mutant cycle *(38)*.

Anti-ssDNA combining sites have been shown to be filled with four to five thymine bases *(10, 39−41)*. Nevertheless, $(dT)_{15}$ was chosen as a ligand here based on the saturation of the dependence of K_a on the length of oligo(dT) (Figure 1). The observed limit in K_a values for $N \geq 15$ likely reflected the influence of both an increase in the number of potential binding sites *(42)* and changes in the entropic contribution of cation release because of the difference in counterion density *(43)*.

van't Hoff Analysis of the Interaction of DNA-1 and HCDR3 Mutants with $(dT)_{15}$. The temperature dependencies of K_a were analyzed in the form of van't Hoff plots (Figure 2) to determine the values of $\Delta H°$ accompanying Fab interaction with $(dT)_{15}$. Linear dependencies of ln K_a versus $1/T$ were observed for all Fab, indicating little change in heat capacity and, therefore, an absence of significant conforma-

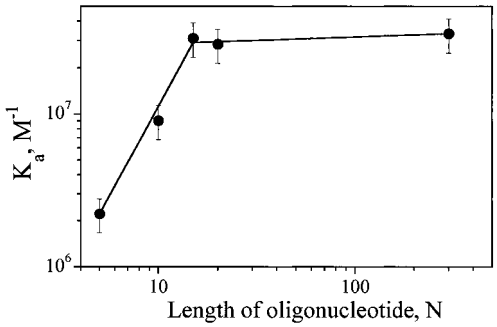

FIGURE 1: Dependence of the association constant (K_a), for the DNA-1−oligo(dT) complex, on the number of bases (N) in the oligonucleotide. The K_a values were measured by fluorescence quenching titration (*19*) in 50 mM Tris-HCl, pH 7.0, at 25 °C.

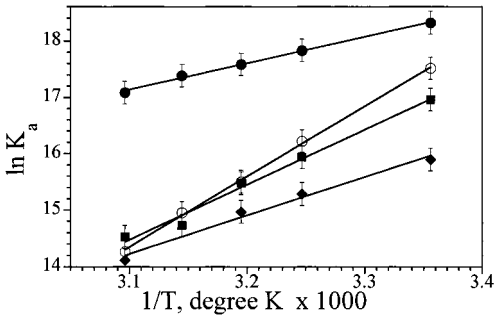

FIGURE 2: van't Hoff plots for the Fab forming a double mutant cycle: DNA-1 (○), R98A (◆), D108A (●), and R98A/D108A (■). All measurements were performed in 50 mM Tris-HCl, pH 7.0, under temperatures ranging from 25 to 50 °C. The temperature dependence of pK_a for Tris was corrected as described under Materials and Methods. The values of $\Delta H°$ were calculated for each Fab from slopes of van't Hoff dependencies and are shown in the Table 1.

tional changes upon Fab−$(dT)_{15}$ complex formation. The $\Delta H°$ values obtained from the slopes of the van't Hoff plots were negative and varied from −9.3 kcal/mol (D108A) to −32.1 kcal/mol (R102T) (Table 1). The $\Delta G°$ and $-T\Delta S°$ values were calculated as described under Materials and Methods and are shown in Table 1. Values of $\Delta G°$, $\Delta H°$, and $-T\Delta S°$ for DNA-1 were −10.4, −24.8, and 14.3 kcal/mol, respectively, reflecting the enthalpic nature of interaction with $(dT)_{15}$. Binding of the oligonucleotide to mutant Fab was also exothermic with negative $T\Delta S°$. The only exception was D108A, demonstrating both favorable $\Delta H°$ and $T\Delta S°$ (Table 1). The changes in $\Delta G°$ ($\Delta\Delta G°$), $\Delta H°$ ($\Delta\Delta H°$), and $-T\Delta S°$ [$\Delta(-T\Delta S°)$], relative to DNA-1, were calculated to determine the impact of alterations in HCDR3 on the thermodynamics of ssDNA binding. The values of $\Delta\Delta H°$ and $\Delta(-T\Delta S°)$, induced by a single amino acid substitution, varied from −7.3 to 15.5 kcal/mol, and from 9.9 to −15.9 kcal/mol, respectively (Table 1). Hence, minor variations in HCDR3 could affect the affinity of Fab−oligonucleotide interactions through changes in the enthalpy−entropy balance in $\Delta G°$.

Enthalpy−Entropy Compensation. Analysis of the data shown in Table 1 revealed that $\Delta\Delta G°$ obtained for all mutants correlated with neither $\Delta\Delta H°$ nor $\Delta(-T\Delta S°)$ and was at least 1 order less in magnitude than the enthalpy and entropy changes. The observed linear relationship between $\Delta H°$ and $(-T\Delta S°)$ with a slope close to unity (0.95) (Figure 3) is a hallmark of complete enthalpy−entropy compensation *(44)*. Extrapolation of the dependence of $\Delta H°$ versus $-T\Delta S°$ to $\Delta H° = 0$, a combining site interacting strictly by a favorable change in the binding entropy (not shown), revealed a $\Delta G°$ of -10.5 ± 0.4 kcal/mol [$K_a = (0.3-1) \times 10^8\ M^{-1}$], which may represent the theoretical limit in affinity to $(dT)_{15}$ for anti-ssDNA Fab originating from DNA-1.

In accordance with the $\Delta\Delta H°$ and $\Delta(-T\Delta S°)$ values, all Fab were divided into two groups: entropy- or enthalpy-driven (Figure 3). The maximal increase in binding entropy was induced by both point mutants directed to the base of HCDR3 (D108A and R98A) (Table 1). Negative $\Delta(-T\Delta S°)$ were also found for three Fab with mutations at the top of HCDR3 (Y101H, Y104H, R102M) and both of the double mutants (R98A/D108A and R102A/P103R) (Table 1). Increased binding entropy may have resulted from either enhanced complex flexibility or increased release of water *(45)* or cations *(35, 46)* from the interacting surfaces of the Fab and oligonucleotide.

All enthalpy-driven Fab (Figure 3) contained mutations at the top of HCDR3 and exhibited an increase in $\Delta G°$ in relation to DNA-1, due to the prevalence of unfavorable $\Delta(-T\Delta S°)$ compared to the decrease in $\Delta H°$ (Table 1). A rise in the exothermicity of Fab−$(dT)_{15}$ interactions was likely due to formation of additional hydrogen bonds and/or changes in the number of ionic pairs at the Fab−ligand interface, that rendered the complex less flexible.

Analysis of Salt Dependencies of the Binding of DNA-1 and HCDR3 Mutants to $(dT)_{15}$. The study of the dependencies of anti-ssDNA Fab affinity on cation concentration could provide information on the role of electrostatic interactions in Fab−ssDNA complex formation *(35, 36, 46, 47)*. Affinities of DNA-1 (Figure 4) and all HCDR3 mutants (Table 2) to $(dT)_{15}$ were found to decrease with increasing cation concentration, indicative of the formation of ionic pairs between Fab and ligand. The slope of a double-logarithmic plot of K_a versus the cation concentration [$d(\ln K_a)/d(\ln [Cat^+])$] (Figure 4) has been shown to equal $-Z\Psi$ *(35, 36)*, where Z is the number of electrostatic contacts formed at the protein−DNA interface and Ψ is the average number of cations released into solution upon formation of each ionic pair. The Ψ value was likely the same for $(dT)_{15}$ when interacting with similar Fab such as DNA-1 and the HCDR3 mutants. The number of ionic pairs formed between $(dT)_{15}$ and DNA-1 and its variants was estimated (Table 2) using $\Psi = 0.76$ attained for a poly(dT)/oligolysine model (*36, 37, 47*). None of the mutants exhibited a decrease in Z, supporting our previous suggestion that HCDR3 interacts with the oligonucleotide bases rather than with the sugar−phosphate backbone *(29)*.

The favorable entropic contribution of cation release to $\Delta G°$ has been predicted to be negligible at a standard cation concentration of 1 M *(35, 36)*. Therefore, extrapolation of the salt dependence to 1 M allowed for the calculation of $\Delta G°_{1M}$ for each Fab which is independent of Ψ (Table 2). Assuming that $\Delta G°_{1M}$ is comprised of $\Delta G°$ of nonelectrostatic interactions ($\Delta G°_{nonel}$) and the free energy of ionic pairs, values of $\Delta G°_{nonel}$ for DNA-1 and HCDR3 mutants were also calculated as $\Delta G°_{1M} + 0.1Z$ (Table 2) (*37, 47*). A linear correlation of $\Delta G°_{nonel}$ with Z (Figure 5) expressed the balance between ionic and nonelectrostatic interactions at the anti-ssDNA combining site. Interestingly, the limited data available for other anti-ssDNA Abs interacting with oligo(dT) (*39, 41, 48*) agreed well with the linear dependence

Table 1: Thermodynamic Parameters of the Interactions between $(dT)_{15}$ and DNA-1 and HCDR3 Mutant Variants[a]

Fab	ΔG^{o},[b] kcal/mol	ΔH^{o},[c] kcal/mol	$-T\Delta S^{o}$,[d] kcal/mol	$\Delta\Delta G^{o}$,[e] kcal/mol	$\Delta\Delta H^{o}$,[e] kcal/mol	$\Delta(-T\Delta S^{o})$,[e] kcal/mol
DNA-1	-10.4 ± 0.1	-24.8 ± 0.3	14.3 ± 0.3	0.0	0.0	0.0
R98A	-9.6 ± 0.2	-13.5 ± 0.6	3.9 ± 0.6	0.8 ± 0.2	11.3 ± 0.6	-10.4 ± 0.6
D108A	-10.9 ± 0.2	-9.3 ± 0.3	-1.6 ± 0.3	-0.5 ± 0.2	15.5 ± 0.3	-15.9 ± 0.3
R98A/D108A	-10.0 ± 0.2	-19.4 ± 0.6	9.3 ± 0.6	0.4 ± 0.2	5.4 ± 0.6	-5.0 ± 0.6
Y101H	-10.1 ± 0.3	-21.6 ± 1.2	11.5 ± 1.2	0.3 ± 0.3	3.2 ± 1.2	-2.8 ± 1.2
Y101N	-9.5 ± 0.3	-24.1 ± 1.1	14.5 ± 1.1	0.9 ± 0.3	0.7 ± 1.1	0.2 ± 1.1
Y101D	-8.1 ± 0.2	-28.5 ± 0.7	20.4 ± 0.7	2.3 ± 0.2	-3.7 ± 0.7	6.1 ± 0.7
R102K	-10.2 ± 0.3	-30.6 ± 1.6	20.4 ± 1.6	0.2 ± 0.3	-5.8 ± 1.6	6.1 ± 1.6
R102M	-10.1 ± 0.3	-21.1 ± 2.0	11.0 ± 2.0	0.3 ± 0.3	3.7 ± 2.0	-3.3 ± 2.0
R102T	-7.9 ± 0.3	-32.1 ± 1.8	24.2 ± 1.8	2.5 ± 0.3	-7.3 ± 1.8	9.9 ± 1.8
P103G	-9.9 ± 0.2	-29.8 ± 1.1	19.9 ± 1.1	0.5 ± 0.2	-5.0 ± 1.1	5.6 ± 1.1
P103T	-9.7 ± 0.2	-29.0 ± 0.4	19.3 ± 0.4	0.7 ± 0.2	-4.2 ± 0.4	5.0 ± 0.4
P103R	-10.0 ± 0.3	-25.7 ± 1.2	15.7 ± 1.2	0.4 ± 0.3	-0.9 ± 1.2	1.4 ± 1.2
R102A/P103R	-8.4 ± 0.3	-17.7 ± 0.6	9.30 ± 0.6	2.0 ± 0.3	7.1 ± 0.6	-5.0 ± 0.6
Y104F	-9.9 ± 0.3	-27.5 ± 1.8	17.7 ± 1.8	0.5 ± 0.3	-2.7 ± 1.8	3.4 ± 1.8
Y104H	-10.1 ± 0.2	-22.1 ± 0.7	12.0 ± 0.7	0.3 ± 0.2	2.7 ± 0.7	-2.3 ± 0.7
Y105F	-9.9 ± 0.2	-29.1 ± 0.9	19.2 ± 0.9	0.5 ± 0.2	-4.3 ± 0.9	4.9 ± 0.9

[a] All experiments were carried out in 50 mM Tris-HCl, pH 7.0, using direct and salt-back fluorescence quenching titration as described under Materals and Methods. [b] Calculated for all Fab studied as $-RT \ln K_a$ where K_a was the association constant of Fab$-(dT)_{15}$ complexes measured at 25 °C. [c] Calculated from the slopes of van't Hoff plots (Figure 2). The temperature of the reaction mixtures ranged from 25 to 50 °C. The temperature dependence of pK_a of Tris was corrected using the coefficient -0.031 pH unit/deg (*34*). [d] Calculated as $\Delta G^{o} - \Delta H^{o}$. [e] Calculated as the difference between corresponding parameters for mutant Fab and DNA-1.

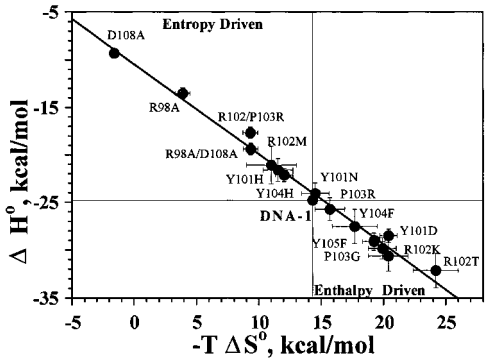

FIGURE 3: Enthalpy−entropy compensation plot for DNA-1 and HCDR3 mutants. Values of ΔH^{o} and $-T\Delta S^{o}$ are shown in Table 1. Fab were divided into enthalpy- or entropy-driven in accordance with favorable changes in ΔH° and $-T\Delta S^{\circ}$. All data were fit to a linear regression equation: $\Delta H^{\circ} = -10.0 + 0.95\ (-T\Delta S^{\circ})$ ($r = 0.99$).

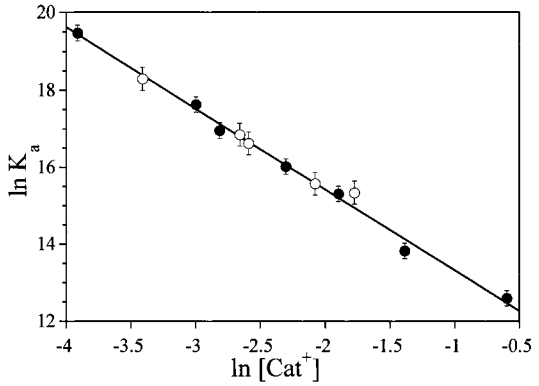

FIGURE 4: Salt dependence of DNA-1: double-logarithmic plot of the K_a of the DNA-1$-(dT)_{15}$ complex versus the total cation concentration ([Cat$^+$]). The K_a values were measured by direct (●) and salt-back (○) fluorescence quenching titration at 25 °C. The line was the best fit of the equation: $\ln K_a = 11.2 - 2.2 \ln [Cat^+]$ ($r = 0.99$). The slope $d(\ln K_a)/d(\ln [Cat^+])$ of the line was equal to $-Z\psi$, where Z was the number of ionic pairs formed between the oligonucleotide and the Fab, and ψ was the number of cations released into solution upon formation of one ionic pair. For DNA-1, Z was calculated as 2.9 ± 0.1 assuming a ψ of 0.76 (*36*, *37*). The value of $\Delta G^{\circ}_{1M} = -RT \ln K_a^{0}$ was calculated as -6.8 ± 0.1 kcal/mol, from the intercept of the fitted line. Similar analyses were also performed for all HCDR3 mutant variants of DNA-1. The data obtained are shown in Table 2.

found for DNA-1 and its variants (Figure 5). The value of ΔG°_{min} (-11.0 kcal/mol) obtained by extrapolation to zero Z could represent the affinity of Fab associating with ssDNA only through nonelectrostatic interactions. From this, the limit in affinity in 1 M salt for anti-ssDNA Fab was estimated as $(1-2) \times 10^{8}$ M^{-1}.

DISCUSSION

Comparison of the Thermodynamics of ssDNA and dsDNA Binding. Overall negative ΔH° values were obtained for DNA-1 and all HCDR3 mutants complexed with $(dT)_{15}$ (Table 1). The exothermicity of DNA-1$-(dT)_{15}$ interactions was confirmed by direct calorimetric measurements (Komissarov et al., unpublished data). Negative $T\Delta S^{\circ}$ values were observed for the majority of Fab studied, reflecting an enthalpic basis of ssDNA binding and a significant stabilization of the combining site domains and the oligonucleotide molecule.

A comparison of the thermodynamics of anti-ssDNA Fab with those of anti-dsDNA Abs Jel 274 and 241 *(15)* promoted an understanding of the molecular mechanisms of DNA−Ab association. Despite similar affinities for antigens and linear van't Hoff plots under low cation concentration, a comparison of ΔH° and $T\Delta S^{\circ}$ values revealed a reciprocal relationship in the forces governing ssDNA and dsDNA binding. In contrast to DNA-1, the association of dsDNA with Jel 274 and Jel 241 was driven strictly by increased binding entropy with positive or unchanged enthalpy *(15)*. The number of ionic pairs formed between ligand and Jel 274 has been shown to be twice higher than that for DNA-1 (*15*). Thus, the entropic nature of interactions at the anti-dsDNA combining site could be a result of the synergistic actions of polyelectrolytic and hydrophobic effects. Hence, the dramatic alterations in the balance of forces governing complex formation may reflect a thermodynamic basis for

Table 2: Analysis of Salt Dependencies of Affinity of DNA-1 and HCDR3 Mutants to $(dT)_{15}$[a]

Fab	Z[b]	ΔZ[c]	ΔG^{o}_{1M},[d] kcal/mol	$\Delta\Delta G^{o}_{1M}$,[c] kcal/mol	ΔG^{o}_{nonel},[e] kcal/mol	$\Delta\Delta G^{o}_{nonel}$,[c] kcal/mol
DNA-1	2.9 ± 0.1	0.0	−6.8 ± 0.1	0.0	−6.5 ± 0.3	0.0
R98A	3.8 ± 0.3	0.9 ± 0.3	−4.3 ± 0.2	2.5 ± 0.2	−3.9 ± 0.4	2.6 ± 0.4
D108A	3.1 ± 0.3	0.2 ± 0.3	−6.5 ± 0.2	0.3 ± 0.2	−6.2 ± 0.3	0.3 ± 0.3
R98A/D108A	3.7 ± 0.1	0.8 ± 0.1	−5.0 ± 0.2	1.8 ± 0.2	−4.6 ± 0.4	1.9 ± 0.4
Y101H	4.2 ± 0.4	1.3 ± 0.4	−4.4 ± 0.3	2.4 ± 0.3	−4.0 ± 0.4	2.5 ± 0.4
Y101N	4.0 ± 0.4	1.1 ± 0.4	−3.9 ± 0.4	2.9 ± 0.4	−3.5 ± 0.4	3.0 ± 0.4
Y101D	3.1 ± 0.4	0.2 ± 0.4	−3.7 ± 0.4	3.1 ± 0.4	−3.4 ± 0.4	3.1 ± 0.4
R102K	2.9 ± 0.3	0.0 ± 0.3	−6.2 ± 0.4	0.6 ± 0.4	−5.9 ± 0.4	0.6 ± 0.4
R102M	3.0 ± 0.3	0.1 ± 0.3	−6.0 ± 0.3	0.8 ± 0.3	−5.7 ± 0.3	0.8 ± 0.3
R102T	3.3 ± 0.4	0.4 ± 0.4	−3.5 ± 0.4	3.3 ± 0.4	−3.2 ± 0.4	3.3 ± 0.4
P103G	4.0 ± 0.3	1.1 ± 0.3	−4.5 ± 0.3	2.3 ± 0.3	−4.1 ± 0.4	2.4 ± 0.3
P103T	3.1 ± 0.3	0.2 ± 0.3	−5.5 ± 0.3	1.3 ± 0.3	−5.1 ± 0.3	1.4 ± 0.3
P103R	4.0 ± 0.3	1.1 ± 0.3	−4.5 ± 0.3	2.3 ± 0.3	−4.1 ± 0.4	2.4 ± 0.4
R102A/P103R	4.2 ± 0.1	1.3 ± 0.1	−2.6 ± 0.2	4.2 ± 0.2	−2.2 ± 0.4	4.3 ± 0.4
Y104F	3.5 ± 0.4	0.6 ± 0.4	−5.1 ± 0.3	1.7 ± 0.3	−4.7 ± 0.4	1.8 ± 0.4
Y104H	4.1 ± 0.3	1.2 ± 0.3	−4.5 ± 0.2	2.3 ± 0.2	−4.1 ± 0.4	2.4 ± 0.4
Y105F	3.1 ± 0.4	0.2 ± 0.4	−5.7 ± 0.3	1.1 ± 0.3	−5.4 ± 0.3	1.1 ± 0.3

[a] Values of K_a were measured in 50 mM Tris-HCl, pH 7.0, with different amounts of NaCl added at 25 °C, using fluorescence quenching titration *(29)*. [b] Calculated as $[-d(\ln K_a)/d(\ln [Cat^+])]/0.76$ *(36, 37)*. [c] Calculated as the difference in values between Fab and DNA-1. [d] Calculated as $-RT \ln K_a^0$, where K_a^0 was the association constant at 1 M cation concentration. [e] Calculated as $\Delta G^{o}_{1M} + 0.1Z$ *(37, 47)*.

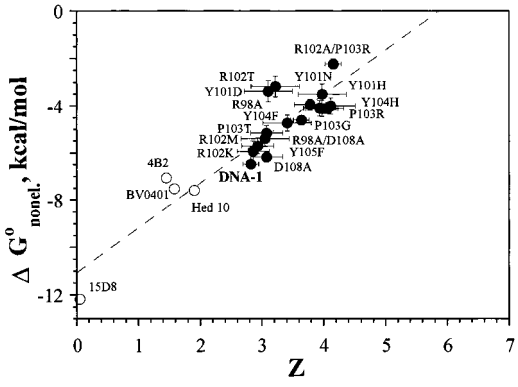

FIGURE 5: Balance of ionic/nonelectrostatic interactions at the anti-ssDNA combining site. Correlation between $\Delta G°_{nonel}$ and the number of ionic pairs formed at the Fab−ligand interface (Z) for DNA-1 and HCDR3 mutants (●) and other anti-ssDNA Abs (○). The values of Z were calculated from the slopes of the salt dependencies as $[-d(\ln K_a)/d(\ln [Cat^+])]/0.76$ *(36, 37)* and $\Delta G°_{nonel}$ as $\Delta G°_{1M} + 0.1Z$ *(37, 47)* (Table 2). The values of Z and $\Delta G°_{nonel}$ for Fab Hed10 (*39*) and Abs 4B2, 15D8 (*41*), and BV04-01 (*48*) were estimated from published data. Salt dependencies were measured by fluorescence quenching titration (20 °C) for Hed10 (*39*), and by gel shift analysis at 4 °C after equilibration at 22 °C for 4B2, 15D8 (*41*), and BV04-01 (*48*). The best fit of the data had a slope of 1.9 kcal/mol per one ionic pair and an intercept of −11.0 kcal/mol ($r = 0.92$).

the recognition of different species of DNA at the combining site.

Interestingly, the *E. coli* ssDNA-binding protein (SSB) also demonstrated both a linear van't Hoff plot and an enthalpy-driven interaction with poly(dT) *(49−51)*. A detailed analysis of the thermodynamics of binding of different oligonucleotides to SSB *(50, 51)* confirmed the suggestion that the specificity of different ssDNA-binding proteins to oligo(dT) can be attributed to the maximal degree of base unstacking for this ligand *(52)*.

Substitution of Residues at the Base of HCDR3 Resulted in Increased Binding Entropy. The residues at the ends of HCDR3 are usually buried and not involved in direct ligand contacts *(25, 53)*. Nevertheless, the engineering of charged residues at the ends of HCDR3 can alter affinity *(29, 44, 54−57)*. Three mutant Fab (R98A, D108A, and R98A/D108A), along with DNA-1, formed a thermodynamic cycle *(38)*, and were analyzed to determine the role of charged residues at the base of HCDR3. In contrast to results obtained for anti-lysozyme (*54*) and anti-carbohydrate (*44*) Abs, all three mutant variants of DNA-1 exhibited a significant increase in $T\Delta S°$ (Table 1). Fab D108A demonstrated the maximal increase in $T\Delta S°$ (15.9 kcal/mol) and had no change in Z, indicating that polyelectrolytic effects did not contribute significantly to the rise in entropy. Therefore, the observed improved affinity of D108A was likely driven either by an increase in the conformational freedom of the complex formed or by hydrophobic effects. Both R98A and R98A/D108A exhibited a decrease in affinity in comparison with DNA-1, despite expected favorable entropic contribution of cation release. Simultaneous substitution of both Arg^{98} and Asp^{108} with alanine resulted in a decrease in $\Delta H°$, compared to the single mutants R98A or D108A, indicating the possible formation of new interactions at the Fab/oligonucleotide interface. Additivity of the changes in $\Delta G°$ demonstrated that Arg^{98} and Asp^{108} likely do not interact with each other under physiological cation concentration. Arg^{98} and Asp^{108} may support the conformation of the combining site and may control interaction patterns such that engineering of the residues at the ends of the HCDR3 loop may serve as the basis for the alteration in the specificity of anti-DNA Fab.

Residues at the Top of HCDR3: ^{101}Tyr-Arg-Pro-Tyr-Tyr^{105}. Six Fab with point mutations and one with a double mutation were designed to probe the role of Pro^{103} and Arg^{102} in binding ssDNA. All single mutations at position 103 exhibited a positive $\Delta(-T\Delta S°)$ and a corresponding increase in $\Delta\Delta G°$. Substitution of Pro^{103} with glycine resulted in a reduction of $T\Delta S°$ by 5.6 kcal/mol, despite the positive entropic contribution of the polyelectrolytic effect ($\Delta Z = 1.1$). In comparison with P103G, P103T displayed a small change in $\Delta G°$ but a decrease in both $\Delta G°_{1M}$ by 1.0 kcal/mol and Z by 1. This improved affinity coincided with the expected favorable contribution of nonelectrostatic interactions ($\Delta Z = -1$). Mutation P103R provoked a further increase in $\Delta H°$ and $T\Delta S°$ and a rise of Z by 1, when compared with P103T. The double mutant R102A/P103R did not exhibit a change in Z compared to P103R. Hence,

Fab P103R, that contains two arginines in a row, likely forms an additional ionic pair with the ligand through Arg^{103} rather than Arg^{102}. The Fab R102K, R102M, and R102T mutants did not exhibit a significant change in *Z*. Therefore, Arg^{102} is likely not involved in direct electrostatic interaction with ligand as had been suggested for anti-dsDNA combining sites *(57)*. Mutations R102T and R102K were accompanied by a significant decrease in $T\Delta S°$ indicating a possible role of Arg^{102} in the maintenance of the conformation of HCDR3 or the combining site as a whole. Analyses of high-resolution structures of the anti-dsDNA Fab Jel 72 and the anti-triple-stranded DNA Fab Jel 318 have directly supported a structural role for arginines in HCDR3 *(11, 12)*.

The three tyrosine residues surrounding Pro^{103} in HCDR3 of DNA-1 have been suggested to participate in $(dT)_{15}$ interaction *(29)*. Substitutions of Tyr^{101} and Tyr^{104} with histidine resulted in almost identical $\Delta\Delta G°$, $\Delta\Delta G°_{1M}$, and ΔZ values, demonstrating that these mutations had a similar impact on the mechanism of ligand binding (Tables 1and 2). Positive $\Delta\Delta H°$ values observed for Y101H and Y104H indicated a possible disruption of interactions at the Fab−ligand interface. The effects of tyrosine/phenylalanine substitutions at positions 101 and 104 were different from those of tyrosine/histidine. Mutation Y101F exhibited more than a 100-fold decrease in affinity to $(dT)_{15}$ (*29)*. The identical values of $\Delta\Delta G°$ obtained for Y104F and Y105F indicated that positions 104 and 105 of HCDR3 are more tolerant than position 101 to the hydrophobic side chain of phenylalanine.

Two mutants, Y101N and Y101D, represented a pair of structurally very similar Fab. However, the isosteric substitution of the amido group with carboxylate was accompanied by a decrease in *Z* by 1, a significant loss in the binding entropy, and an increase in $\Delta G°$ by 1.4 kcal/mol (Table 1). Comparable $\Delta\Delta G°_{nonel}$ values (Table 2) apparently signified similar patterns of nonelectrostatic interactions for these Fab. The contribution to $\Delta G°$ by one ionic pair at the Fab−(dT_{15}) interface calculated in 50 mM Tris-HCl buffer (1.4 kcal/mol per one ionic pair) can reflect the potential for formation of nonspecific protein−DNA complexes of high affinity under low cation concentrations.

Balance of Ionic−Nonelectrostatic Interactions at the Anti-ssDNA Combining Site. The complexity of changes in the thermodynamics induced by the mutations was illustrated by a lack of correlation between the positive entropic contribution expected from an increase in *Z* and the change in $T\Delta S°$ obtained for R102T, P103G, P103R, and Y104F. The balance in ionic/nonelectrostatic interactions at the anti-ssDNA combining site could, however, be expressed as the dependence of $\Delta G°_{nonel}$ versus *Z* (Figure 5). An explanation for the linear relationship may be due to comparable interface areas of different anti-ssDNA Fab and the similarity in the thermodynamic contribution of ionic interactions through phosphoryl groups. It should be noted that the three mutant Fab with the maximal positive $\Delta\Delta G°$ and $\Delta\Delta G°_{1M}$ values (Y101D, R102T, and R102A/P103R) deviated the greatest from the best-fit curve (Figure 5), perhaps due to changes in their interface areas.

The value of $\Delta G°_{min}$ estimated for the anti-ssDNA combining site free of ionic interactions shown in Figure 5 (−11.0 kcal/mol) was close to that estimated from the enthalpy−entropy compensation plot (Figure 3) and the $\Delta G°$ reported for Fab 15D8, whose affinity to $(dT)_{21}$ was shown to be independent of salt concentration *(41)*. The slope of the dependence of $\Delta G°_{nonel}$ versus *Z* was equal to 1.9 kcal/mol, and likely reflects the energetic price for substitution of the part of the combining site occupied by nonelectrostatic interactions with one ionic pair. This value was close to that determined for the contribution of one methylene group (−1.4 kcal/mol) to the $\Delta G°$ of substrate binding for an aromatic amino acid aminotransferase *(58)*. Extrapolation to $\Delta G°_{nonel} = 0$ (Figure 5) would represent a Fab interacting with ligand only via electrostatic interactions. Thus, the maximal number of ionic pairs at the Fab−ssDNA interface (Z_{max}) was estimated as 6−7. Using the van der Waals radius or the buried area of a phosphoryl group determined from X-ray crystallographic data *(59)*, along with Z_{max}, an average Fab−ssDNA contact area was estimated to be 450−550 Å^2. The interface areas of BV04-01/$(dT)_3$ (*10*) as well as other Ab−antigen complexes *(13)* that were determined from X-ray data were in agreement with this value. The specific $\Delta G°$ of nonelectrostatic interaction calculated from $\Delta G°_{min}$ and the interface area was found to range from −20 to −25 cal/(mol·Å^2). The specific $\Delta G°$ of nonelectrostatic interaction directly measured for the anti-lysozyme Ab D1.3 (*60*), and reported for other Abs (*61*), was similar to that found for anti-ssDNA Fab.

Data reported in this study demonstrated that minor changes in the structure of HCDR3 were able to induce alterations in the affinity and potentially the specificity of the anti-ssDNA combining site through changes in the balances in entropy−enthalpy to $\Delta G°$ or in electrostatic−nonionic interactions. These results will assist in interpretation of X-ray crystallographic data currently being collected for DNA-1 and attempts at the rational engineering of the anti-DNA combining site.

ACKNOWLEDGMENT

We thank Rene Matthews for his expert help in Fab purification, Marie Marchbank in manuscript preparation, and Mike Henzl, Thomas Quinn, and Jack Tanner for their valuable comments.

REFERENCES

1. Chothia, C., and Lesk, A. M. (1987) *J. Mol. Biol. 196*, 901−917.
2. Schwartz, R. S., and Stollar, B. D. (1985) *J. Clin. Invest. 75*, 321−332.
3. Tan, E. M. (1989) *Adv. Immunol. 44*, 93−152.
4. Pisetsky, D. S., Grudier, J. P., and Gilkenson, G. S. (1990) *Arth. Rheum. 33*, 153−159.
5. Winfield, J. B., Faiferman, I., and Koffler, D. (1991) *J. Clin. Invest. 59*, 90−95.
6. Swanson, P. C., Yung, R. L., Blatt, N. B., Eagan, M. A., Norris, J. M., Richardson, B. C., Johnson, K. J., and Glick, G. D. (1996) *J. Clin. Invest. 97*, 1748−1760.
7. Eilat, D., and Anderson, W. F. (1994) *Mol. Immunol. 31*, 1377−1390.
8. Barry, M. M., Mol, C. D., Anderson, W. F., and Lee, J. S. (1994) *J. Biol. Chem. 269*, 3623−3632.
9. Cygler, M., Boodhoo, A., Lee, J. S., and Anderson, W. F. (1987) *J. Biol. Chem. 262*, 643−648.
10. Herron, J. N., He, X. M., Ballard, D. W., Blier, P. R., Pace, P. E., Bothwell, A. L. M., Voss, E. W., Jr., and Edmundson, A. B. (1991) *Proteins: Struct., Funct., Genet. 11*, 159−175.
11. Mol, C. D., Muir, A. K. S., Lee, J. S., and Anderson, W. F. (1994) *J. Biol. Chem. 269*, 3605−3614.

12. Mol, C. D., Muir, A. K. S., Cygler, M., Lee, J. S., and Anderson, W. F. (1994) *J. Biol. Chem. 269*, 3615−3622.
13. Padlan, E. A. (1994) *Mol. Immunol. 31*, 169−217.
14. Nadassy, K., Wodak, S. J., and Janin, J. (1999) *Biochemistry 38*, 1999−2017.
15. Tanha, J., and Lee, J. S. (1997) *Nucleic Acids Res. 25*, 1442−1449.
16. Gulliver, G. A., Bedzyk, W. D., Smith, R. G., Bode, S. L., Tetin, S. Y., and Voss, E. W. (1994) *J. Biol. Chem. 269*, 7934−7940.
17. Gulliver, G. A., Rumbley, C. A., Carrero, J., and Voss, E. W., Jr. (1995) *Biochemistry 34*, 5158−5163.
18. Calcutt, M. J., Komissarov, A. A., Marchbank, M. T., and Deutscher, S. L. (1996) *Gene 168*, 9−14.
19. Komissarov, A. A., Calcutt, M. J., Marchbank, M. T., Peletskaya, E. N., and Deutscher, S. L. (1996) *J. Biol. Chem. 271*, 12241−12246.
20. Barbas, S. M., Ditzel, H. J., Salonen, E. M., Yang, W., Silverman, G. J., and Burton, D. R. (1995) *Proc. Natl. Acad. Sci. U.S.A. 92*, 2529−2533.
21. Pewzner-Jung, Y., Simon, T., and Eilat, D. (1996) *J. Immunol. 154*, 2198−2208.
22. Barbas, S. M., Ghazal, P., Barbas, C. F., III, and Burton, D. R. (1994) *J. Am. Chem. Soc. 116*, 2161−2162.
23. Chothia, C., Lesk, A. M., Tramontano, A., Levitt, M., Smith-Gill, S., Air, G., Sheriff, S., Padlan, E., Davies, D., Tulip, W., Colman, P., Spinelli, S., Alzari, P., and Poljak, R. (1989) *Nature 342*, 877−883.
24. Al-Lazikani, B., Lesk, A. M., and Chothia, C. (1997) *J. Mol. Biol. 273*, 927−948.
25. Morea, V., Tramontano, A., Rustici, M., Chothia, C., and Lesk, A. M. (1998) *J. Mol. Biol. 275*, 269−294.
26. Calcutt, M. J., Kremer, M. T., Giblin, M. F., Quinn, T. P., and Deutscher, S. L., (1993) *Gene 137*, 77−83.
27. Deutscher, S. L., Crider, M. E., Ringbauer, J., Komissarov, A. A., and Quinn, T. P. (1996) *Arch. Biochem. Biophys. 333*, 207−213.
28. Komissarov, A. A., Marchbank, M. T., and Deutscher, S. L. (1997) *Anal. Biochem. 247*, 123−129.
29. Komissarov, A. A., Marchbank, M. T., Calcutt, M. J., Quinn, T. P., and Deutscher, S. L. (1997) *J. Biol. Chem. 272*, 26864−26870.
30. Laemmli, U. K. (1971) *Nature 227*, 680−685.
31. Smith, P. K., Krohn, R. I., Hermanson, G. T., Mallia, A. K., Gartner, F. H., Provenzano, M. D., Fujimoto, E. K., Goeke, N. M., Olson, B. J., and Klenk, D. C. (1985*) Anal. Biochem. 150*, 76−85.
32. Overman, L. B., Bujalowski, W., and Lohman, T. M. (1988) *Biochemistry 27*, 456−471.
33. Lohman, T. M., and Mascotti, D. P. (1992) *Methods Enzymol. 212*, 424−458.
34. Good, N. E., Winget, G. D., Winter, W., Connolly, T. N., Izava, S., and Singh, R. M. (1966) *Biochemistry 5*, 467−477.
35. Record, M. T., Lohman, T. M., and De Haseth, P. L. (1976) *J. Mol. Biol. 107*, 145−158.
36. Record, M. T., Jr., Woodbury, C. P., and Lohman, T. M. (1976) *Biopolymers 15*, 893−915.
37. Mascotti, D. P., and Lohman, T. M. (1993) *Biochemistry 32*, 10568−10579.
38. Carter, P. J., Winter, G., Wilkinson, A. J., and Fersht, A. R. (1984) *Cell 38*, 835−840.
39. Lee, J. S., Dombroski, D. F., and Mosmann, T. R. (1982) *Biochemistry 21*, 4940−4945.
40. Rumbley, C. A., Denzin, L. K., Yantz, L., Tetin, S. Yu., and Voss, E. W., Jr. (1993) *J. Biol. Chem. 268*, 13667−13674.
41. Swanson, P. C., Ackroyd, C., and Glick, G. D. (1996) *Biochemistry 35*, 1624−1633.
42. McGhee, J. D., and von Hippel, P. H. (1974) *J. Mol. Biol. 86*, 469−489.
43. Zhang, W., Bond, J. P., Anderson, C. F., Lohman, T. M., and Record, M. T., Jr. (1996) *Proc. Natl. Acad. Sci. U.S.A. 93*, 2511−2516.
44. Brummell, D. A., Sharma, V. P., Anand, N. N., Bilous, D., Dubic, G., Michniewicz, J., MacKenzie, C. R., Sadowska, J., Sigurskjold, B. W., Sinnott, B., Young, N. M., Bundle, D. R., and Narang, S. A. (1993) *Biochemistry 32*, 1180−1187.
45. Sturtevant, J. M. (1977) *Proc. Natl. Acad. Sci. U.S.A. 74*, 2236−2240.
46. De Haseth, P. L., Lohman, T. M., and Record, M. T. (1977) *Biochemistry 16*, 4783−4790.
47. Lohman, T. M., and Mascotti, D. P. (1992) *Methods Enzymol. 212*, 400−424.
48. Swanson, P. C., Copper, B. C., and Glick, G. D. (1994) *J. Immunol. 152*, 2601−2612.
49. Lohman, T. M., and Ferrari, M. E. (1994) *Annu. Rev. Biochem. 63*, 527−570.
50. Ferrari, M. E., and Lohman, T. M. (1994) *Biochemistry 33*, 12896−12910.
51. Kozlov, A. G., and Lohman, T. M. (1999) *Biochemistry 38*, 7388−7397.
52. Sang, B., and Gray, D. M. (1989) *J. Biomol. Struct. Dyn. 7*, 693−706.
53. Satow, Y., Cohen, G., Padlan, E. A., and Davies, D. R. (1986) *J. Mol. Biol. 190*, 593−604.
54. Panka, D. J., Mudgett-Hunter, M., Parks, D. R., Peterson, L. L., Herzenberg, L. A., Haber, E., and Margolies, M. N. (1988) *Proc. Natl. Acad. Sci. U.S.A. 85*, 3080−3084.
55. Chien, N. C., Roberts, V. A., Giusti, A. M., Scharff, M. D., and Getzoff, E. D. (1989) *Proc. Natl. Acad. Sci. U.S.A. 86*, 5532−5536.
56. Ito, W., Iba, Y., and Kurosawa, Y. (1993) *J. Biol. Chem. 268*, 16639−16647.
57. Radic, M. Z., Mackle, J., Erikson, C., Mol, W. F., and Weigert, M. (1993) *J. Immunol. 150*, 4966−4977.
58. Kawaguchi, S., and Kuramitsu, S. (1998) *J. Biol. Chem. 273*, 18353−18364.
59. Barford, D., Hu, S.-H., and Johnson, L. N. (1991) *J. Mol. Biol. 218*, 233−260.
60. Ysern, X., Fields, B. A., Bhat, T. N., Goldbaum, F. A., Dall'Acqua, W., Schwarz, F. P., Poljak, R. J., and Mariuzza, R. A. (1994) *J. Mol. Biol. 238*, 496−500.
61. Chothia, C. (1974) *Nature 248*, 338−339.

BI991347L